

## Optimum RF Pulse Width for Adiabatic Bloch-Siegert $B_1^+$ Mapping

Mohammad Mehdi Khalighi<sup>1</sup>, Adam B Kerr<sup>2</sup>, and Brian K Rutt<sup>3</sup>

<sup>1</sup>Applied Science Lab, GE Healthcare, Menlo Park, California, United States, <sup>2</sup>Department of Electrical Engineering, Stanford University, Stanford, California, United States, <sup>3</sup>Department of Radiology, Stanford University, Stanford, California, United States

**Purpose:** The Adiabatic Bloch-Siegert (ABS)  $B_1^+$  mapping method [1] addresses the long TE and high RF power deposition (SAR) problems of conventional B-S pulses [2] by introducing short frequency-swept ABS pulses with maximum sensitivity, which in turn allows for much faster B-S  $B_1^+$  mapping within approved SAR limits. However, it is still not clear how to design the optimal ABS pulse for a given pulse sequence; by optimal, we mean the highest Angle to Noise Ratio (ANR) in the resulting  $B_1^+$  maps. In this work we present a method to optimize ABS pulse design; we first optimize the analytically designed ABS pulse and then we extend this theory to numerically optimized ABS pulses.

**Theory:** The ABS pulse that produces maximum Bloch-Siegert phase shift ( $\Delta\phi_{BS}$ ) with a given pulse width ( $T$ ) and peak amplitude ( $B_{1p}$ ) is defined by Eq. (1-3), where  $K$  (adiabatic factor) is a design parameter which determines the in-band excitation tolerance [1]. In a special case where there is no  $B_0$  inhomogeneity, the B-S shift is given by Eq. (4). Assuming large  $K$  values and relatively short pulses and using a Taylor expansion of Eq. (4), the B-S phase shift can be approximated by Eq. (5). Assuming that the sequence is always run with maximum allowable SAR in order to get highest ANR, the amplitude of the ABS pulse is given by Eq. (6), where  $K_s$  is a constant factor. In order to compare ABS pulses with different pulse widths, we define ABS pulse efficiency,  $\Gamma$ , as the ABS phase shift adjusted by the SNR hit due to  $T_2^*$  signal decay caused by the echo time increase that results from the insertion of the ABS pulse into the pulse sequence. Combining Eqs. (5) and (6),  $\Gamma$  is given by Eq. (7), where  $K_T$  are all the terms in  $\Delta\phi_{BS}$  which are independent of ABS pulse width,  $T$ . By setting  $d\Gamma/dT = 0$  the optimum pulse width which maximizes  $\Gamma$  is found in Eq. (8), which is equal to  $\frac{3}{4}T_2^*$ .

**Methods:** A numerically optimized ABS pulse was designed with -40 dB in-band attenuation assuming  $\pm 500$  Hz on-resonance bandwidth. The ABS pulse was inserted into a spiral sequence for

B-S  $B_1^+$  mapping. The spiral sequence parameters were selected as minimum TE, minimum TR, 2048 points, 2 arms, bandwidth  $\pm 83.3$  kHz, FOV 24 cm, slice thickness 5 mm, flip angle 30 deg and 25 contiguous slices. The sequence was used on a 7T GE scanner (GE Healthcare, Waukesha, WI) using a 32ch Nova Head coil (Nova Medical, Wilmington, MA). Based on the SAR limit, the peak amplitude ( $B_{1p}$ ) values for 27 different ABS pulses with various pulse widths  $T$  in the range 1-14 ms with 0.5 ms step were calculated for minimum TR. The B-S phase shift of each pulse was calculated using a Bloch simulation and the efficiency of each pulse was obtained from Eq. (7) for  $T_2^*$  values over the range of [1 30] ms. A subject was scanned and the  $B_1^+$  map was acquired using 2, 4 and 6 ms ABS pulses. The scan was repeated 20 times for each pulse and ANR maps were generated.

**Results:** Fig. 1 shows the ABS pulse amplitude and phase modulation profiles along with the transverse magnetization frequency response, which is plotted for the 4ms numerically optimized ABS pulse. Fig. 2 shows the B-S pulse efficiency plotted as a function of  $T$  and  $T_2^*$  showing how the pulse efficiency decreases as  $T_2^*$  decreases. The efficiency of longer ABS pulses decreases faster due to the longer echo time. The pulses that create the maximum efficiency for each  $T_2^*$  value were picked from Fig. 2 and those optimal pulse widths vs.  $T_2^*$  are plotted in Fig. 3. For comparison the optimum pulse width for the analytical design (Eq. 8) is also plotted (blue line) and a good match with the numerically designed ABS pulse width vs.  $T_2^*$  behavior is observed, with slope equal to  $\frac{3}{4}$ . As  $T_2^*$  is variable around the brain, 2, 4 and 6 ms pulses were chosen for ANR comparison in head at 7T. Fig. 4 compares the ANR obtained by these 3 pulses. It shows that the 6ms ABS pulse is the most efficient under the same scan-time and SAR constraint.

**Discussion:** For maximum B-S  $B_1^+$  mapping efficiency, we designed ABS pulses with minimum TR achievable by the spiral sequence and showed high quality  $B_1^+$  maps at 7T for head. The optimum ABS pulse width depends on  $T_2^*$ . We showed that in head at 7T, 6ms ABS pulse generates very high quality  $B_1^+$  maps.

**References:** [1]Khalighi et al., MRM DOI 10.1002/mrm.24507. [2]Sacolic et al., MRM 63:1315-1322, 2010.

**Acknowledgement:** Research support from GE Healthcare. Grant support from NIH P41 EB015891.

$$\begin{aligned}
 (1) \quad B_1(t) &= \Pi\left(\frac{t-T/2}{T}\right) e^{i\Delta\omega(t)} \\
 (2) \quad \Delta\omega(t) &= \begin{cases} \gamma B_{1p} \cot \psi & 0 < t < T/2 \\ \gamma B_{1p} \cot(\psi - \psi_0) & T/2 < t < T \end{cases} \\
 (3) \quad \psi(t) &= \cos^{-1}\left(1 - \frac{\gamma B_{1p} T}{K}\right), \quad \psi_0 = \psi\left(\frac{T}{2}\right) \\
 (4) \quad \Delta\phi_{BS} &= 4K(\psi_0 - \sin \psi_0) \\
 (5) \quad \Delta\phi_{BS} &\approx \frac{2(\gamma B_{1p} T)^{3/2}}{3K^{1/2}} \\
 (6) \quad B_{1p} &= \sqrt{\frac{K_s TR}{T}} \\
 (7) \quad \Gamma &= \Delta\phi_{BS} e^{-T/T_2^*} = K_T T^{3/4} e^{-T/T_2^*} \\
 (8) \quad T_{opt} &= \frac{3}{4} T_2^*
 \end{aligned}$$

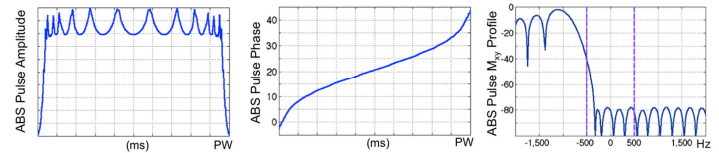


Fig. 1: ABS pulse amplitude and phase along with transverse magnetization profile for the 4ms ABS pulse.

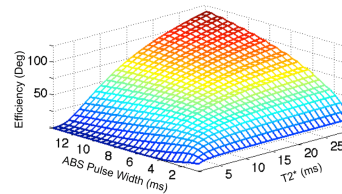


Fig. 2: ABS pulse efficiency of numerically designed ABS pulses with different  $T_2^*$  value.

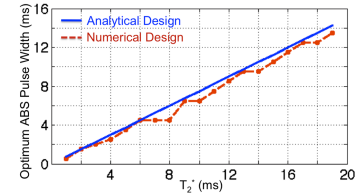


Fig. 3: Optimum ABS pulse width with different  $T_2^*$  values using numerical & analytical methods.

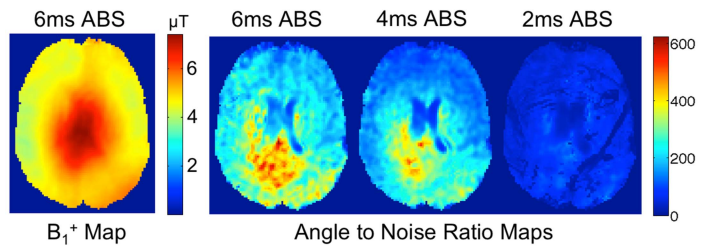


Fig. 4: ANR maps of brain  $B_1^+$  map (left) acquired with ABS using 2, 4 and 6ms pulse widths.